



# London Dispersion Favors Sterically Hindered Diarylthiourea Conformers in Solution

Lars Rummel<sup>+</sup>, Marvin H. J. Domanski<sup>+</sup>, Heike Hausmann, Jonathan Becker, and Peter R. Schreiner<sup>\*</sup>

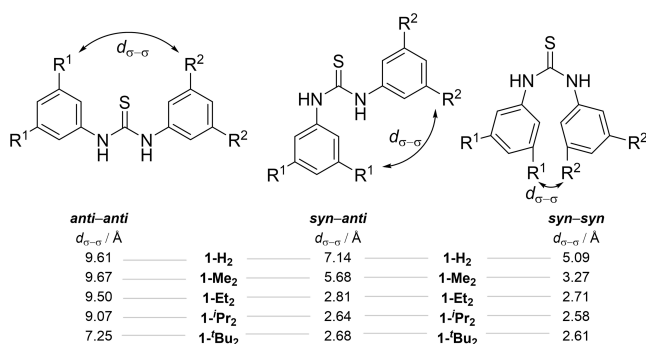
**Abstract:** We present an experimental and computational study on the conformers of *N,N'*-diphenylthiourea substituted with different dispersion energy donor (DED) groups. While the unfolded *anti-anti* conformer is the most relevant for thiourea catalysis, intramolecular noncovalent interactions counterintuitively favor the folded *syn-syn* conformer, as evident from a combination of low-temperature nuclear magnetic resonance measurements and computations. In order to quantify the noncovalent interactions, we utilized local energy decomposition analysis and symmetry-adapted perturbation theory at the DLPNO-CCSD(T)/def2-TZVPP and sSAPT0/6-311G(d,p) levels of theory. Additionally, we applied a double-mutant cycle to experimentally study the effects of bulky substituents on the equilibria. We determined London dispersion as the key interaction that shifts the equilibria towards the *syn-syn* conformers. This preference is likely a factor why such thiourea derivatives can be poor catalysts.

## Introduction

In the field of enzyme catalysis, Fischer's "key and lock" hypothesis<sup>[1]</sup> or the more sophisticated "induced fit" model by Koshland<sup>[2]</sup> perennially highlight the importance of conformational flexibility and catalytic activity. The structural dynamics of peptides allow enzymes to bind and to recognize substrates effectively and convert them into products. Thus, a specific conformer of the catalyst is needed to exploit transition state stabilization and energetic differ-

entiation among a series of possible transition state geometries. Conformational structure–property relationships can be probed with small molecules as well. The restricted bond rotation within the thioamide functional group offers three differently populated conformers (Scheme 1).<sup>[3]</sup> While the mechanism for anion recognition or catalytic activation of a substrate due to hydrogen-bonding is most effective via the open *anti-anti* conformer, an analysis of the conformational landscape of thiourea derivatives is an essential part to understand the origin of their catalytic activity and any limitations thereof.<sup>[3]</sup> Here, we present a study of *all-meta*-disubstituted diphenylthiourea<sup>[4]</sup> derivatives to elucidate the conformational preferences dependent on noncovalent interactions including London dispersion (LD).<sup>[5]</sup> Since the compounds discussed in this work both are less catalytically active than commonly exploited thiourea catalysts<sup>[4c]</sup> and poor anion receptors,<sup>[4b,6]</sup> we hypothesize this is in part due to the population of a conformer that does not allow double N–H bonding to Lewis-basic atoms or groups in the substrate.<sup>[3]</sup>

In recent years, a number of studies demonstrated that the catalytically active *anti-anti* diphenyl(thio)urea conformer is not necessarily the predominant conformer in the gas phase and in solution.<sup>[3,6a, 7]</sup> Infrared and temperature-dependent NMR measurements in different solvents demonstrated the presence of multiple conformers for diarylthiourea derivatives.<sup>[7]</sup> An exception to this conformational flexibility is the well-known *N,N'*-bis[3,5-bis(trifluoromethyl)phenyl]thiourea catalyst with the *anti-anti* conformer being predominant in, for example, tetrahydrofuran (THF)



**Scheme 1.** Lowest energy conformers of diphenylthiourea derivatives with the *anti-anti* (left), *syn-anti* (center), and *syn-syn* (right) conformers. The shown values correspond to the shortest  $\sigma-\sigma$  distance  $d_{\sigma-\sigma}$  contact for each conformer of 1-*R*<sup>1</sup>-*R*<sup>2</sup> computed at B3LYP-D3(BJ)/def2-TZVPP.

[\*] L. Rummel,<sup>+</sup> M. H. J. Domanski,<sup>+</sup> H. Hausmann, P. R. Schreiner  
 Institute of Organic Chemistry, Justus Liebig University  
 Heinrich-Buff-Ring 17, 35392 Giessen (Germany)  
 E-mail: prs@uni-giessen.de

J. Becker  
 Institute of Inorganic and Analytical Chemistry, Justus Liebig  
 University  
 Heinrich-Buff-Ring 17, 35392 Giessen (Germany)

[<sup>+</sup>] These authors contributed equally to this work.

© 2022 The Authors. Angewandte Chemie International Edition published by Wiley-VCH GmbH. This is an open access article under the terms of the Creative Commons Attribution Non-Commercial NoDerivs License, which permits use and distribution in any medium, provided the original work is properly cited, the use is non-commercial and no modifications or adaptations are made.

at elevated temperatures.<sup>[3]</sup> While the experimental evidence points to the fact that the *anti-anti* conformer of this thiourea catalyst is catalytically most active, other substitution patterns are likely to display a different conformational landscape, which, in turn, is likely to result in reduced catalytic activity.

Most recently, Sandler et al.<sup>[6a]</sup> highlighted the relationship of conformational effects and the anion binding affinity of receptor molecules such as diphenylthiourea.<sup>[4h,6b]</sup> Whereas urea and squaramide derivatives prefer the *anti-anti* conformer due to intramolecular CH-carbonyl hydrogen bonding, diphenylthiourea does not benefit as strongly from this stabilization since its phenyl moieties are twisted out of plane.<sup>[4c]</sup> Consequently, diphenylthiourea populates the *syn-anti* and *syn-syn* conformers, thereby lowering its anion binding affinity.<sup>[6a]</sup> To explain the enantioselectivity of an asymmetric Henry reaction, Heshmat proposed cinchonathiourea catalyst substrate activation via the *syn-anti* conformer.<sup>[8]</sup> Experimental data suggest a similar trend. In an extensive study of crystal structures of urea and thiourea derivatives, Luchini et al.<sup>[9]</sup> showed that around 60% of all thiourea motifs crystallize in a *syn-syn* or *syn-anti* fashion. On the other hand, 98% of urea derivatives are reported to have an *anti-anti* conformation in the solid state.<sup>[9]</sup> Solid state and gas phase IR<sup>[10]</sup> and NMR<sup>[11]</sup> studies in solution support this trend for urea derivatives as well. For diarylthiourea derivatives, IR measurements suggest a significant shift to the *syn-syn* conformer in solution<sup>[7]</sup> but a systematic NMR study determining the role and the apparent intramolecular stabilization of the *syn-syn* conformer has not been reported.

In order to investigate the equilibria depicted in Scheme 1, we treated the *N,N'*-diphenylthiourea derivatives as molecular balances.<sup>[12]</sup> By increasing the size of the *all-meta*-substituted aryl dispersion energy donors (DEDs),<sup>[5,13]</sup> we observed a systematic and counterintuitive shift of the equilibrium toward the folded and more crowded *syn-syn* conformer. The increasing number of close  $\sigma$ - $\sigma$  contacts is indicative of the prevalence of attractive LD<sup>[14]</sup> interactions rather than Pauli (exchange) repulsion. This effect was recently emphasized in a study of the equilibria of 1,4- and 1,6-di-*t*-butyl cyclooctatetraene in a large series of solvents of very different polarities showing that intramolecular LD interactions do not cancel in solution.<sup>[15]</sup>

## Results and Discussion

To dissect the influence of each DED, we synthesized a logical series of diphenylthiourea derivatives with methyl (Me), ethyl (Et), *iso*-propyl (*i*Pr), and *tert*-butyl (*t*Bu) substituents. In brief, the *all-meta*-substituted *N,N'*-diphenylthioureas were synthesized via a two-step addition of aniline precursors to thiophosgene.<sup>[3]</sup> Prior, the *all-meta*-substituted aniline precursors were generated via bromination and de-diazotization reaction of 2,6-disubstituted aniline derivatives (for details, see Supporting Information).<sup>[16]</sup> To gather as much information as possible, we generated all R<sup>1</sup> and R<sup>2</sup> combinations of these groups and measured

<sup>1</sup>H NMR spectra in THF. The choice of solvent was based on its physical properties (i.e., low melting point) and the fact that all diphenylthiourea derivatives remained soluble during the low-temperature NMR measurements.

The restricted bond rotation of all *N,N'*-diphenylthiourea derivatives required low-temperature NMR measurements (performed at 193 K) in order to freeze the C–N bond rotation. The lowest temperature possible to hold up over a longer period of time in the NMR was 193 K. Intrinsic barriers of 10.3 kcalmol<sup>-1</sup> (corresponding to a rate constant of 4.0 × 10<sup>-3</sup> s<sup>-1</sup>) and 9.0 kcalmol<sup>-1</sup> (1.3 s<sup>-1</sup>) for unsubstituted diphenylthiourea.<sup>[3]</sup> We first tested our approach with *N,N'*-bis(3,5-di-*tert*-butylphenyl)thiourea **1-*t*Bu<sub>2</sub>** (**1-R<sup>1</sup>R<sup>2</sup>**) and the parent *N,N'*-diphenylthiourea **1-H<sub>2</sub>**. For both derivatives the singlet N–H signal splits into three separate signals upon cooling, two of which belong to the same conformer (blue marking, Figure 1). Additionally, the aromatic signals (Figure 2) split into four, and the aliphatic *tert*-butyl signals into two separate NMR peaks.

Accordingly, these signals were assigned to the *syn-anti* conformer since it is the only structure with inequivalent N–H, aromatic, and *tert*-butyl protons. While the parent **1-H<sub>2</sub>** (purple NMR, Figure 1) considerably favors the *syn-anti* conformer by around 2.3 ± 0.1 kcalmol<sup>-1</sup> (all energies were determined via K<sub>eq</sub> at 193 K), the NMR of **1-*t*Bu<sub>2</sub>**

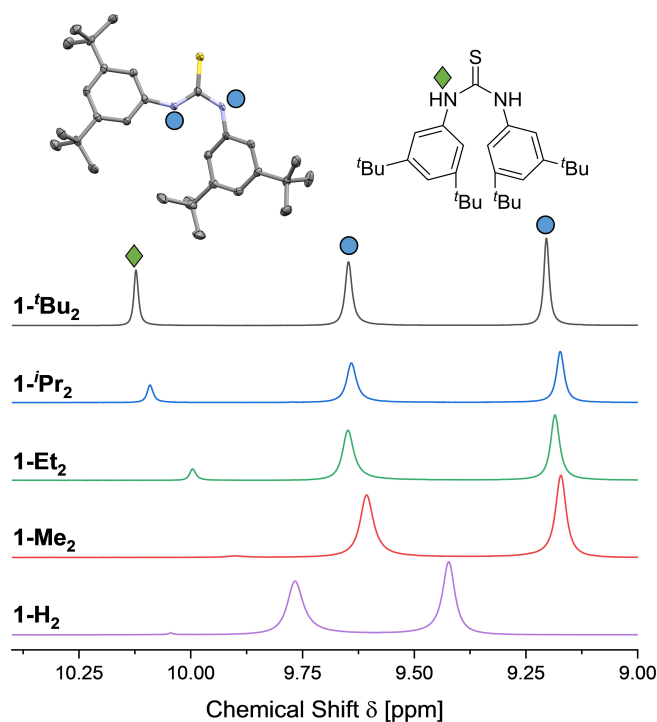


**Figure 1.** NMR measurements at 193 K of symmetrically substituted *N,N'*-diphenylthiourea derivatives **1-R<sup>1</sup>R<sup>2</sup>** in THF and molecular structure of **1-*t*Bu<sub>2</sub>**. For simplicity, the NH signals of symmetric **1-R<sup>1</sup>R<sup>2</sup>** are depicted only. Thermal ellipsoid plot of the molecular structure obtained by single-crystal X-ray diffraction was drawn at 50% probability level. The blue markings correspond to the NH signals of the *syn-anti* and the green markings to the *syn-syn* conformer. Note that the *anti-anti* conformer is not populated and has therefore been omitted.

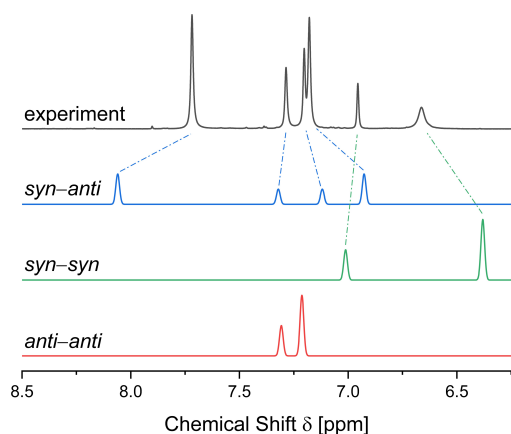


**Figure 2.** NMR measurements at 193 K of the aromatic signals of **1-Bu<sub>2</sub>** (grey) and computed spectra for the *syn-anti* (blue), *syn-syn* (green), and *anti-anti* (red) conformers in THF (SMD solvent model) at the B3LYP-D3(BJ)/def2-TZVPP level of theory. For the full spectral data see the Supporting Information.

(black NMR, Figure 1) shows a distinct symmetric conformer. Nevertheless, **1-Bu<sub>2</sub>** favors the *syn-anti* conformer by around  $0.5 \pm 0.0(3)$  kcal mol<sup>-1</sup>. The computed NMR signals (Figure 2) suggest that the new signals belong to the *syn-syn* conformer (green spectrum), which also helped us assign the *syn-anti* (blue spectrum) and disregard the *anti-anti* (red spectrum) conformer. Whereas the N–H proton shift is difficult to determine by NMR computations,<sup>[17]</sup> the aromatic and aliphatic C–H signals were assigned to the *syn-syn* conformer.

Concentration dependent measurements showed no change in signal ratios with the lowest concentration being 15.5 mM (0.01 mmol). This is in line with NMR measurements investigating the complexation of thiourea catalyst with lactones, where it was found that the *anti-anti* conformer is catalytically most active.<sup>[3]</sup> Consequently, aggregation in solution was deemed to be unimportant. To ensure that equilibrium had been reached, we equilibrated each NMR sample for one hour at 193 K. Since the barrier height for rotation around the thioamide bond is around 10 kcal mol<sup>-1</sup>, equilibrium was reached after around 5 min (see Supporting Information for details). After transferring the samples to the NMR spectrometer, they were further equilibrated until the temperature stabilized at 193 K. Figure 1 displays the N–H proton splitting for symmetric **1-R<sup>1</sup>R<sup>2</sup>**. While **1-H<sub>2</sub>** shows only low concentrations of a second conformer, bulky substituents such as those with *tert*-butyl groups clearly affect the conformer distributions.

Figure 3 displays a summary of the experimentally determined  $\Delta G_{R^1R^2-HH}$  values of the equilibrium between *syn-syn* and *syn-anti* **1-R<sup>1</sup>R<sup>2</sup>** relative to parent *N,N*-diphenylthiourea **1-H<sub>2</sub>**. Consequently, **1-H<sub>2</sub>** is depicted as  $\Delta G_{R^1R^2-HH} = 0.0 \pm 0.2$  kcal mol<sup>-1</sup> in Figure 3 (rightmost data point). While **1-H<sub>2</sub>** favors the *syn-anti* conformer by around  $2.3 \pm 0.1$  kcal mol<sup>-1</sup> (see Supporting Information for absolute energy values), substituents in all-*meta* position shift the equilibrium towards the *syn-syn* conformer ( $\Delta G < 0$ ). In contrast to the often encountered view that large groups

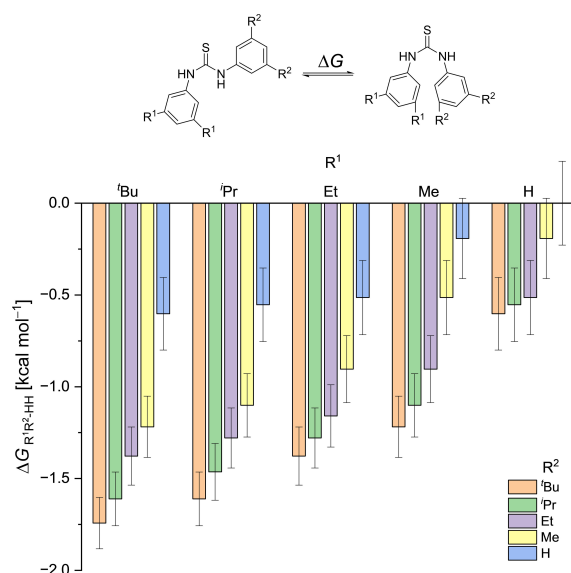


**Figure 3.** Experimentally determined Gibbs free energy values  $\Delta G_{R^1R^2-HH}$  for the equilibrium between *syn-syn* and *syn-anti* **1-R<sup>1</sup>R<sup>2</sup>** at 193 K. Gray lines indicate error bars.  $\Delta G < 0$  corresponds to a shift towards the *syn-syn* conformer: The lower and more negative the  $\Delta G$  expressed, the more favored the *syn-syn* conformer. Note that the supposedly catalytically active *anti-anti* conformation is not populated at all.

repel each other, Figure 3 illustrates that bulky groups favor the conformer that displays close alkyl–alkyl contacts ( $d_{\sigma-\sigma} = 2.61$  Å for **1-Bu<sub>2</sub>**). The *unsymmetric* functionalization in **1-R<sup>1</sup>H** (blue bars) and **1-HR<sup>2</sup>** (rightmost block of columns) only has a small effect on the equilibrium position (up to  $\Delta G_{BuH-HH} = -0.6 \pm 0.2$  kcal mol<sup>-1</sup>). The shift in energy towards the *syn-syn* conformer can be rationalized by attractive  $\sigma-\pi$  interactions between substituents and opposing phenyl moiety. Thereby, a decrease in distance between substituent and phenyl moiety systematically increases the stabilizing  $\sigma-\pi$  interactions. A similar effect was already observed and quantified by Shimizu et al. for a *para* substitution pattern utilizing molecular torsion balance.<sup>[18]</sup> Here, distance dependence of  $\sigma-\pi$  interactions was documented for a *para* substitution pattern with the largest and bulkiest alkyl groups forming the strongest stabilizing interactions. These observations are consistent with the recent concept of DEDs in which bulky alkyl groups form stabilizing dispersion interactions.<sup>[5,13]</sup>

By systematically increasing the substituent size on both phenyl moieties, the equilibrium shifts further to the more crowded *syn-syn* structure. The introduction of additional CH<sub>3</sub> groups increases the number of close intramolecular alkyl–alkyl contacts in the *syn-syn* conformer, thereby reducing the distance between substituents (Scheme 1). An increasing number of noncovalent contacts at distances of around 2.5 Å has proven to be effective in stabilizing labile compounds such as hexaphenylethane<sup>[19]</sup> or rationalizing isomerization energies of linear and branched alkanes.<sup>[20]</sup> The largest difference in energy due to incorporation of a methyl substituent can be observed from **1-BuH** ( $\Delta G$

${}^t\text{BuH-HH} = -0.6 \pm 0.2 \text{ kcal mol}^{-1}$ ) to **1-<sup>t</sup>BuMe** ( $\Delta G_{\text{BuMe-HH}} = -1.2 \pm 0.2 \text{ kcal mol}^{-1}$ ) with around  $-0.6 \text{ kcal mol}^{-1}$  stabilization due to  $\sigma$ - $\sigma$  contacts.<sup>[21]</sup> Additional methyl groups shift the equilibrium further towards the *syn-syn* conformer by around  $-0.1 \text{ kcal mol}^{-1}$ . Consequently, the most prominent effects can be observed for **1-<sup>t</sup>R<sup>1</sup>Bu** derivatives (orange bars), which shift the equilibria significantly towards the *syn-syn* conformer (up to  $\Delta G_{\text{Bu-HH}} = -1.7 \pm 0.1 \text{ kcal mol}^{-1}$ ). Hence, the experimental data suggest that increasingly larger alkyl substituents act as stabilizing DEDs rather than as repulsive steric bulk.<sup>[5,19, 22]</sup> Correlations of our experimental findings with the molecular volume or in the total molecular dipole moment of each conformer are insufficient to rationalize the trends observed (see Supporting Information).

To support these findings, we performed a computational study focusing on the role of intramolecular non-covalent interactions. To be able to switch dispersion corrections on and off, we utilized density functional theory (DFT) to investigate the equilibria depicted in Scheme 1. After an initial conformer analysis using the Conformer-Rotamer Ensemble Sampling Tool<sup>[23]</sup> (crest) program, the lowest conformers were further optimized with Ahlrich's def2-TZVPP<sup>[24]</sup> basis set. The B3LYP<sup>[25]</sup> functional was utilized with and without (Supporting Information) Grimme's D3<sup>[26]</sup> correction including Becke-Johnson<sup>[27]</sup> (BJ) damping. All geometry optimizations were performed in the gas phase under standard conditions. The gas phase structures were utilized for single-point energy computations to account for solvation effects and entropy at 193 K. The polarizable continuum model (PCM)<sup>[28]</sup> was used with THF as solvent and thermal corrections added from DFT (gas phase) frequency computations. Additionally, the B3LYP-D3(BJ) (gas phase) optimized structures were utilized for single-point energy computations at the DLPNO-CCSD(T)/def2-TZVPP level of theory.<sup>[29]</sup> This analysis follows that of Sandler et al. (Supporting Information)<sup>[6a]</sup> who demonstrated that the B3LYP functional in conjunction with medium-sized basis sets is an appropriate approach for geometry optimizations of thiourea derivatives and, that DLPNO-CCSD(T)/large basis set is an excellent approximation to its canonical counterpart. Since LD interactions are in a first approximation temperature independent, the results of the thermochemical analysis of the equilibrium fit qualitatively to gas phase computations (see Supporting Information).<sup>[14]</sup> The thermochemical results ( $\Delta G_{\text{eq}}$ ) for the symmetric and unsymmetric *N,N'*-diphenylthiourea molecular balances are depicted in Figure 4. While the *anti-anti* conformer is highest in energy (red markings) for all systems and cannot be observed by NMR, the *syn-syn* (green markings) conformers are generally favored. Computations on B3LYP/def2-TZVPP excluding the LD corrections predict the *syn-anti/anti-syn* conformers to be favored by around 3–4 kcal mol<sup>-1</sup>. Including LD, the unsubstituted balance already slightly favors the *syn-syn* conformer ( $\Delta G_{\text{eq}} \approx -0.3 \text{ kcal mol}^{-1}$ ). Increasing alkyl substitution shifts the global energy minimum further from the *syn-anti* towards the *syn-syn* conformer. The largest effect can be observed for **1-<sup>t</sup>Bu<sub>2</sub>** ( $\Delta G_{\text{eq}} \approx -2.8 \text{ kcal mol}^{-1}$ ). These results

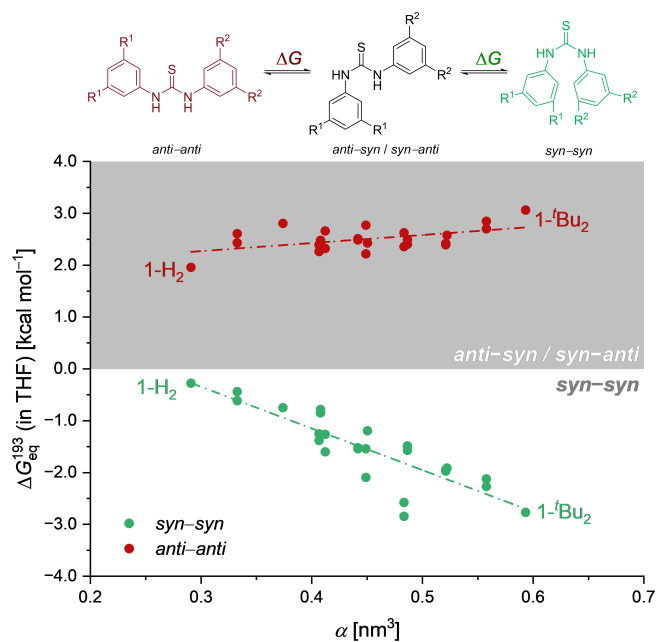


**Figure 4.** Gibbs free energies at 193 K for the equilibrium of the *syn-syn* (green markings) and *anti-anti* (red markings) conformers relative to the *syn-anti/anti-syn* conformers of **1-R<sup>1</sup>R<sup>2</sup>** at the DLPNO-CCSD(T)/def2-TZVPP//B3LYP-D3(BJ)/def2-TZVPP level of theory including a solvent correction (THF) at the B3LYP-D3(BJ)/def2-TZVPP utilizing the PCM model. Thermal corrections were added from DFT optimizations at 193 K. **1-H<sub>2</sub>** and **1-<sup>t</sup>Bu<sub>2</sub>** are highlighted for clarity.

fit qualitatively well to our experimental data, albeit the attenuation of the attractive interactions due to solvent effects is higher than predicted by the computations.<sup>[30]</sup>

To assess these counterintuitive results, we visualized the intramolecular noncovalent contacts (Figure 5) utilizing non-covalent interaction (NCI) plots<sup>[31]</sup> to highlight the main source of thermodynamic stability of **1-<sup>t</sup>Bu<sub>2</sub>** by depicting the reduced density gradient in regions of low electron density. While strongly attractive and repulsive interactions are color-coded in blue and red, respectively, green isosurfaces can be assigned to weak NCIs. The *anti-anti* conformer of **1-<sup>t</sup>Bu<sub>2</sub>** features a mixture of red and blue isosurfaces due to the substitution pattern and a CH...S contact<sup>[4c]</sup> a green contact area is not visible. On the other hand, the *syn-anti* conformer already shows small green areas between bulky <sup>t</sup>Bu substituents and the opposing phenyl group. Finally, the *syn-syn* conformer shows large green isosurfaces implying significant intramolecular NCIs. An incorporation of bulky alkyl groups increases the number of noncovalent contacts via close  $\sigma$ - $\sigma$  (i.e., <sup>t</sup>Bu-<sup>t</sup>Bu in Figure 5) and  $\sigma$ - $\pi$  (<sup>t</sup>Bu- $\pi$ ) contacts of both substituents. This analysis qualitatively supports experimental and computational findings.

To quantify the amount of LD interactions between each substituent, we dissected the energy values  $\Delta\Delta G_{\text{R}^1\text{R}^2}$  from singly substituted molecular balances.<sup>[32]</sup> Hereby, two substituents R<sup>1</sup> and R<sup>2</sup> are mutated separately to investigate the impact of each substituent on the thiourea molecular backbone. According to the following equation the inter-

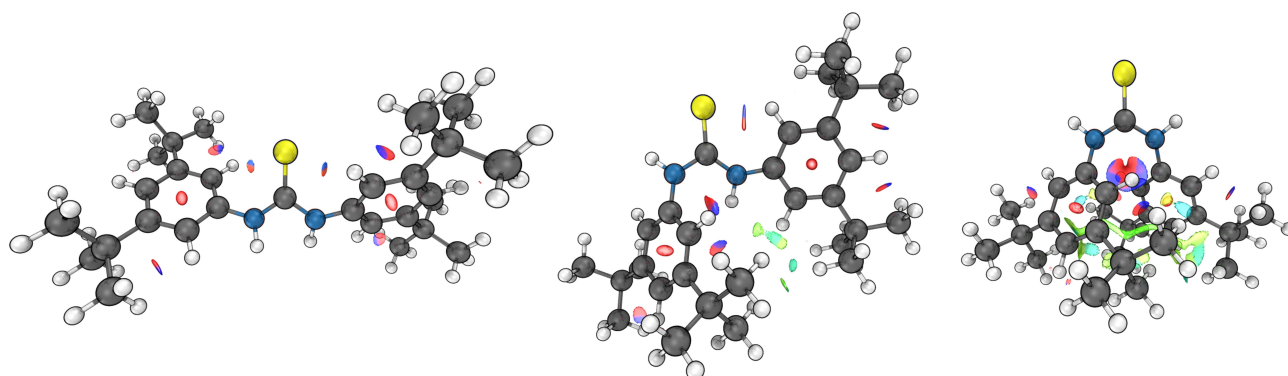


**Figure 5.** Noncovalent interaction (NCI) plots of the *anti-anti* (left), *syn-anti* (center), and *syn-syn* (right) conformers of **1-Bu<sub>2</sub>**, at B3LYP-D3(BJ)/def2-TZVPP. Isosurfaces (isovalue  $s$  of 0.2, ranging from  $\text{sign}(\lambda_2)\rho = -0.05$  a.u. to  $+0.05$  a.u.) are color-coded red (indicating strong repulsion), blue (strong attractive interactions), and green (corresponding to weak NCI).

action energy  $\Delta\Delta G_{R^1R^2}$  between two substituents can be determined as follows:

$$\Delta\Delta G_{R^1R^2} = \Delta G_{R^1R^2} - \Delta G_{R^1H} - \Delta G_{HR^2} + \Delta G_{HH} \quad (1)$$

While this application of Hess's law (also referred to as double mutant cycle) gives an experimental estimate of the role each DED plays, the results have to be treated with caution due to a large error estimate (see Supporting Information for details). Nevertheless, Figure 6 qualitatively supports our findings that sterically hindered diphenylthiourea derivatives favor the *syn-syn* conformer. In general, all calculated energies are negative implying a stabilizing effect between the alkyl groups. Especially for large moieties, a stabilization of the *syn-syn* conformer can be observed ( $\Delta\Delta G_{R^1R^2} = -0.5 \pm 0.3$  kcal mol<sup>-1</sup>). Therefore, around 30% of the observed Gibbs free energy values ( $\Delta\Delta G_{R^1R^2-HH} = -1.7 \pm 0.1$  kcal mol<sup>-1</sup>) can be assigned to stabilizing alkyl-alkyl contacts. The remaining 70% consists of  $\sigma$ - $\pi$  interactions between <sup>t</sup>Bu and the opposing phenyl moiety.<sup>[21]</sup> The smallest effect was measured for the **1-Me<sub>2</sub>** molecular balance ( $\Delta\Delta G_{MeMe} = -0.1 \pm 0.4$  kcal mol<sup>-1</sup>). In comparison to  $\Delta\Delta G_{R^1Me}$  (yellow bars),  $\Delta\Delta G_{R^1Et}$  (purple bars) does not profit from an additional CH<sub>3</sub> group. This can be rationalized with an entropic penalty<sup>[33]</sup> due to increasing flexibility of the ethyl substituent.

With the aim to dissect the intramolecular interaction energy into its main contributors, we employed symmetry-adapted-perturbation theory<sup>[34]</sup> (SAPT) analysis as implemented in PSI4.<sup>[35]</sup> The scaled version was used according to Sherrill et al.<sup>[36]</sup> to improve the performance of the decomposition method. We focused solely on the interaction between the two substituted phenyl moieties. As a starting point, we took the B3LYP-D3(BJ)/def2-TZVPP optimized geometries and removed the thiourea moiety. The resulting phenyl radicals were saturated with hydrogen yielding a benzene dimer in geometry of the *syn-syn*, *syn-anti* and *anti-anti* conformer. This approach allows us to transfer the intramolecular into intermolecular interactions between two substituted benzene molecules. While the electronic substitution of benzene varies from the electronic structure

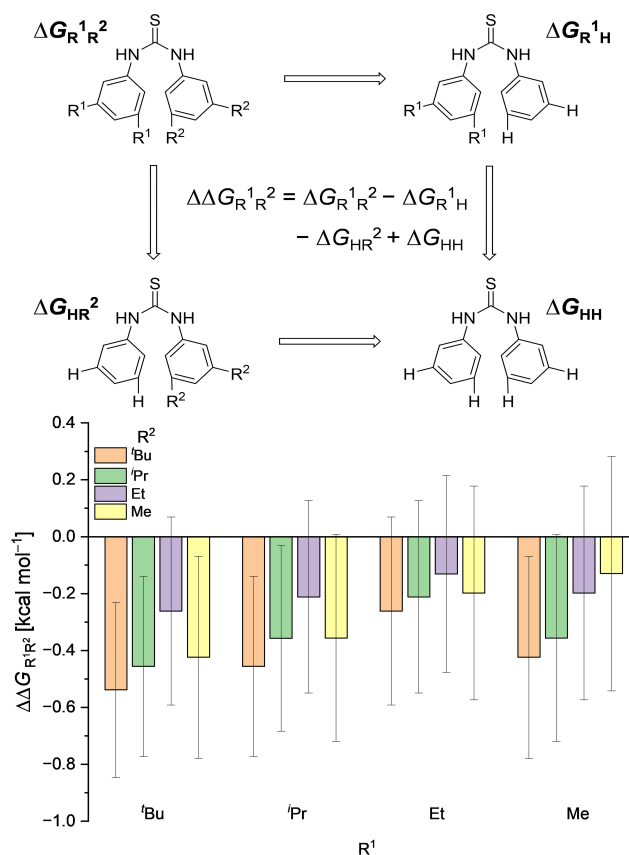


**Figure 6.** Double mutant cycle (top) to dissect the interaction energy  $\Delta\Delta G_{R^1R^2}$  and results of the analysis (bottom); gray lines indicate error bars.  $\Delta\Delta G_{R^1R^2}$  describes the relative interaction energies of  $R^1$ - $R^2$  contacts of the *syn-anti* and *syn-syn* equilibrium at 193 K. Negative energies correspond to stabilizing interactions between both groups.

within diphenylthiourea, this method was solely used to identify the main source of thermodynamic stability. Figure 7 displays the energy decomposition of the total interaction energy ( $E_{\text{tot}}$ ) between two di-substituted benzene molecules based on their geometry in the *syn-syn* conformer (for other conformers see Supporting Information). While inductive effects ( $E_{\text{ind}}$ , blue markings) only play a minor role

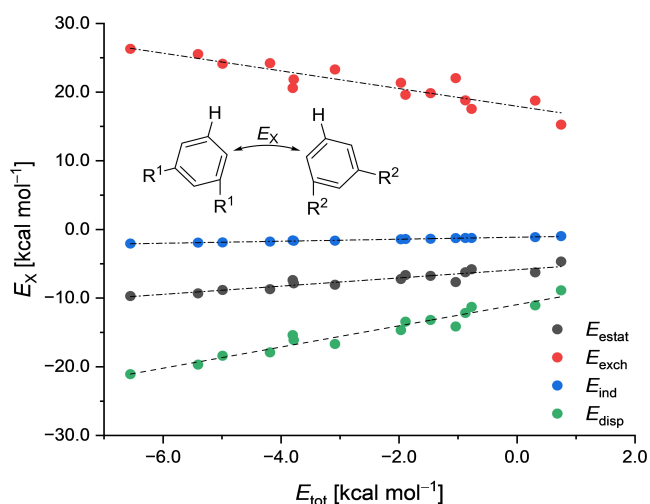


**Figure 7.** sSAPT analysis of two 1,3-disubstituted benzene molecules in the geometry of the *syn-syn* thiourea conformers at sSAPT0/6-311G(d,p) at 298 K. The dashed lines are used to guide the eye.

in the dimerization of substituted benzene, electrostatic ( $E_{\text{estat}}$ , grey markings) as well as LD interaction ( $E_{\text{disp}}$ , green markings) are essential to understand the interaction energy between two benzene molecules. Both energies,  $E_{\text{estat}}$  and  $E_{\text{disp}}$ , stabilize the benzene dimer due to alkyl substitution with LD interactions as the major component (up to  $E_{\text{disp}} = -21.1 \text{ kcal mol}^{-1}$  for **1-Bu<sub>2</sub>**). Nevertheless, only a combination of both energies overcompensates the destabilizing contributions of Pauli exchange repulsion ( $E_{\text{exch}}$ , red markings). Especially for **1-H<sub>2</sub>**, repulsive interactions ( $E_{\text{exch}} = +15.3 \text{ kcal mol}^{-1}$ ) disfavor the aggregation of benzene and override all stabilizing effects ( $E_{\text{tot}} = +0.7 \text{ kcal mol}^{-1}$ ). While Herbert et al.<sup>[37]</sup> identified LD as the main attractive component in cofacial  $\pi$ -stacking (via  $\sigma$ - $\pi$  contacts) of benzene, this effect alone is not strong enough to stabilize **1-H<sub>2</sub>**. The geometry of close benzene dimers enforced through the thiourea molecular backbone is therefore not ideal to afford the perfect balance between attractive and repulsive contacts. With increasing substituent bulkiness repulsive interactions increase (up to  $E_{\text{exch}} = +26.3 \text{ kcal mol}^{-1}$  for **1-Bu<sub>2</sub>**) but do not overcompensate the attractive interactions.

After establishing that LD interactions are the major factor for the conformational preference of diphenylthiourea derivatives, we set out to quantify the magnitude of LD interactions between the aromatic moieties without changing the electronic structure of *N,N'*-diphenylthiourea. While the double mutant cycle (Figure 6) represents the total interaction energy (sum of all attractive and repulsive components) between DED groups attached, the overall energy gain due to LD interactions was dissected using a Local Energy Decomposition (LED) analysis<sup>[38]</sup> as implemented in ORCA.<sup>[39]</sup> Therefore, we fragmented every *N,N'*-diphenylthiourea molecular balance into three parts (F1, F2, and F3). During this process all bonds are cleaved homolytically resulting in large electrostatic interactions between all fragments. Consequently, we investigated only the gain in

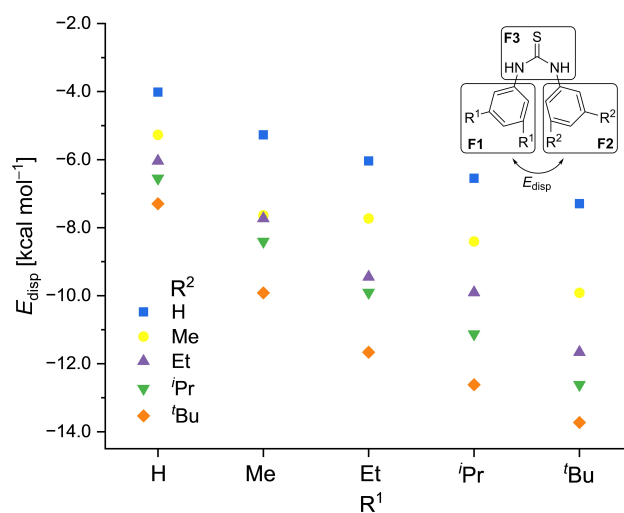


**Figure 8.** LD interaction energies derived from LED analysis of two **1-R<sup>1</sup>R<sup>2</sup>** substituted phenyl moieties in *syn-syn* conformer at DLPNO-CCSD(T)/def-TZVP//B3LYP-D3(BJ)/def2-TZVPP at 298 K.

energy due to LD interactions between F1 and F2. Figure 8 shows the results of the analysis for the *syn-syn* conformers (see Supporting Information for other conformers).

The LED analysis fits qualitatively to the results of computational and experimental data very well. In comparison to the SAPT analysis, LED suggests lower LD contributions (around  $6 \text{ kcal mol}^{-1}$ ), but this is due to the different models used. Accordingly, **1-H<sub>2</sub>** and the semi-substituted **1-HR<sup>2</sup>** series benefit the least from LD interactions (between  $-4.0$  to  $-7.3 \text{ kcal mol}^{-1}$ ). On the other hand, substitution on both phenyl moieties results in higher LD interaction energies up to  $E_{\text{disp}} = -13.7 \text{ kcal mol}^{-1}$  for **1-Bu<sub>2</sub>**. This effect is most prominent in the *syn-syn* conformer. All methods utilized to quantify noncovalent interactions demonstrate the role of LD on the conformational preference of *N,N'*-diphenylthiourea derivatives. The experimental and computational data suggest simple additivity of the DED strength due to an increasing preference of the *syn-syn* conformer with growing steric bulk. The double mutant cycle highlights both,  $\sigma$ - $\sigma$  and  $\sigma$ - $\pi$  contacts as the origin of stabilization.

## Conclusion

We performed a systematic experimental-computational study on the folding equilibria of all-*meta* substituted diphenylthiourea derivatives investigating the impact of steric bulk on the conformer preferences. In stark contrast to the broadly accepted dominance of Pauli repulsion dictating conformations, we identified LD interactions as the main contributor that counterintuitively stabilizes the *syn-syn* conformers. Therefore, LD proves to be a powerful interaction to shift equilibria towards apparently *more crowded* conformers.

A double-mutant cycle allowed us to quantify and differentiate between attractive  $\sigma$ - $\sigma$  and  $\sigma$ - $\pi$  contacts as

origin of stabilization. The most prominent shift towards the folded *syn-syn* conformer was observed when attaching bulky *tert*-butyl substituents to diphenylthiourea. An SAPT analysis reveals a combination of electrostatic and LD interactions counteracting Pauli repulsion. The LED analysis helped quantify intramolecular LD interactions and confirmed *tert*-butyl substituents to be highly effective DEDs.

### Acknowledgements

This work was supported by the priority program “Control of London Dispersion in Molecular Chemistry” (SPP1807) of the Deutsche Forschungsgemeinschaft. We thank Jan M. Schümann for fruitful discussions. Open Access funding enabled and organized by Projekt DEAL.

### Conflict of Interest

The authors declare no conflict of interest.

### Data Availability Statement

The data that support the findings of this study are available in the Supporting Information of this article.

**Keywords:** Conformational Analysis · Local Energy Decomposition · Pauli Repulsion · Symmetry-Adapted-Perturbation Theory ·  $\sigma$ - $\sigma$  Interactions

- 
- [1] E. Fischer, *Ber. Dtsch. Chem. Ges.* **1894**, 27, 2985–2993.  
 [2] D. E. Koshland, *Proc. Natl. Acad. Sci. USA* **1958**, 44, 98.  
 [3] K. M. Lippert, K. Hof, D. Gerbig, D. Ley, H. Hausmann, S. Guenther, P. R. Schreiner, *Eur. J. Org. Chem.* **2012**, 5919–5927.  
 [4] a) P. R. Schreiner, A. Wittkopp, *Org. Lett.* **2002**, 4, 217–220; b) P. R. Schreiner, *Chem. Soc. Rev.* **2003**, 32, 289–296; c) A. Wittkopp, P. R. Schreiner, *Chem. Eur. J.* **2003**, 9, 407–414; d) Y. Takemoto, *Org. Biomol. Chem.* **2005**, 3, 4299–4306; e) S. J. Connon, *Chem. Eur. J.* **2006**, 12, 5418–5427; f) M. S. Taylor, E. N. Jacobsen, *Angew. Chem. Int. Ed.* **2006**, 45, 1520–1543; *Angew. Chem.* **2006**, 118, 1550–1573; g) A. G. Doyle, E. N. Jacobsen, *Chem. Rev.* **2007**, 107, 5713–5743; h) Z. Zhang, P. R. Schreiner, *Chem. Soc. Rev.* **2009**, 38, 1187–1198.  
 [5] J. P. Wagner, P. R. Schreiner, *Angew. Chem. Int. Ed.* **2015**, 54, 12274–12296; *Angew. Chem.* **2015**, 127, 12446–12471.  
 [6] a) I. Sandler, F. A. Larik, N. Mallo, J. E. Beves, J. Ho, *J. Org. Chem.* **2020**, 85, 8074–8084; b) F. Dressler, P. R. Schreiner in *Anion–Binding Catalysis* (Ed.: O. G. Mancheño), Wiley-VCH, Weinheim, **2022**, pp. 1–77.  
 [7] B. Galabov, G. Vassilev, N. Neykova, A. Galabov, *J. Mol. Struct.* **1978**, 44, 15–21.  
 [8] M. Heshmat, *J. Phys. Chem. A* **2018**, 122, 7974–7982.  
 [9] G. Luchini, D. M. H. Ascough, J. V. Alegre-Requena, V. Gouverneur, R. S. Paton, *Tetrahedron* **2019**, 75, 697–702.  
 [10] a) R. Emery, N. A. Macleod, L. C. Snoek, J. P. Simons, *Phys. Chem. Chem. Phys.* **2004**, 6, 2816–2820; b) H. M. Badawi, W. Förner, *Spectrochim. Acta Part A* **2012**, 95, 435–441.  
 [11] L. V. Sudha, D. N. Sathyanarayana, S. N. Bharati, *Magn. Reson. Chem.* **1987**, 25, 474–479.  
 [12] a) S. Paliwal, S. Geib, C. S. Wilcox, *J. Am. Chem. Soc.* **1994**, 116, 4497–4498; b) I. K. Mati, S. L. Cockroft, *Chem. Soc. Rev.* **2010**, 39, 4195–4205; c) M. A. Strauss, H. A. Wegner, *Eur. J. Org. Chem.* **2019**, 295–302.  
 [13] S. Grimme, R. Huenerbein, S. Ehrlich, *ChemPhysChem* **2011**, 12, 1258–1261.  
 [14] a) F. London, *Z. Phys.* **1930**, 63, 245–279; b) F. London, *Trans. Faraday Soc.* **1937**, 33, 8b–26.  
 [15] J. M. Schümann, J. P. Wagner, A. K. Eckhardt, H. Quanz, P. R. Schreiner, *J. Am. Chem. Soc.* **2021**, 143, 41–45.  
 [16] C. Eschmann, L. Song, P. R. Schreiner, *Angew. Chem. Int. Ed.* **2021**, 60, 4823–4832; *Angew. Chem.* **2021**, 133, 4873–4882.  
 [17] H. C. Da Silva, W. B. De Almeida, *Chem. Phys.* **2020**, 528, 110479.  
 [18] J. Hwang, P. Li, M. D. Smith, K. D. Shimizu, *Angew. Chem. Int. Ed.* **2016**, 55, 8086–8089; *Angew. Chem.* **2016**, 128, 8218–8221.  
 [19] S. Rösel, C. Balestrieri, P. R. Schreiner, *Chem. Sci.* **2017**, 8, 405–410.  
 [20] a) K. S. Pitzer, *J. Chem. Phys.* **1955**, 23, 1735–1735; b) K. S. Pitzer, E. Catalano, *J. Am. Chem. Soc.* **1956**, 78, 4844–4846.  
 [21] a) M. Alonso, T. Woller, F. J. Martín-Martínez, J. Contreras-García, P. Geerlings, F. De Proft, *Chem. Eur. J.* **2014**, 20, 4931–4941; b) A. A. Fokin, D. Gerbig, P. R. Schreiner, *J. Am. Chem. Soc.* **2011**, 133, 20036–20039.  
 [22] a) L. Schweighauser, M. A. Strauss, S. Bellotto, H. A. Wegner, *Angew. Chem. Int. Ed.* **2015**, 54, 13436–13439; *Angew. Chem.* **2015**, 127, 13636–13639; b) G. Lu, R. Y. Liu, Y. Yang, C. Fang, D. S. Lambrecht, S. L. Buchwald, P. Liu, *J. Am. Chem. Soc.* **2017**, 139, 16548–16555.  
 [23] P. Pracht, F. Bohle, S. Grimme, *Phys. Chem. Chem. Phys.* **2020**, 22, 7169–7192.  
 [24] A. Schäfer, C. Huber, R. Ahlrichs, *J. Chem. Phys.* **1994**, 100, 5829–5835.  
 [25] a) C. Lee, W. Yang, R. G. Parr, *Phys. Rev. B* **1988**, 37, 785–789; b) A. D. Becke, *J. Chem. Phys.* **1993**, 98, 5648–5652.  
 [26] S. Grimme, J. Antony, S. Ehrlich, H. Krieg, *J. Chem. Phys.* **2010**, 132, 154104.  
 [27] S. Grimme, S. Ehrlich, L. Goerigk, *J. Comput. Chem.* **2011**, 32, 1456–1465.  
 [28] a) S. Miertuš, E. Scrocco, J. Tomasi, *Chem. Phys.* **1981**, 55, 117–129; b) J. Tomasi, B. Mennucci, R. Cammi, *Chem. Rev.* **2005**, 105, 2999–3094.  
 [29] a) C. Riplinger, F. Neese, *J. Chem. Phys.* **2013**, 138, 034106; b) D. G. Liakos, M. Sparta, M. K. Kesharwani, J. M. L. Martin, F. Neese, *J. Chem. Theory Comput.* **2015**, 11, 1525–1539.  
 [30] a) L. Yang, C. Adam, G. S. Nichol, S. L. Cockroft, *Nat. Chem.* **2013**, 5, 1006–1010; b) R. Pollice, M. Bot, I. J. Kobylanski, I. Shenderovich, P. Chen, *J. Am. Chem. Soc.* **2017**, 139, 13126–13140.  
 [31] a) E. R. Johnson, S. Keinan, P. Mori-Sánchez, J. Contreras-García, A. J. Cohen, W. Yang, *J. Am. Chem. Soc.* **2010**, 132, 6498–6506; b) J. Contreras-García, E. R. Johnson, S. Keinan, R. Chaudret, J.-P. Piquemal, D. N. Beratan, W. Yang, *J. Chem. Theory Comput.* **2011**, 7, 625–632.  
 [32] a) P. J. Carter, G. Winter, A. J. Wilkinson, A. R. Fersht, *Cell* **1984**, 38, 835–840; b) H. Adams, F. J. Carver, C. A. Hunter, J. C. Morales, E. M. Seward, *Angew. Chem. Int. Ed. Engl.* **1996**, 35, 1542–1544; *Angew. Chem.* **1996**, 108, 1628–1631.  
 [33] a) D. Van Craen, W. H. Rath, M. Huth, L. Kemp, C. Räuber, J. M. Wollschläger, C. A. Schalley, A. Valkonen, K. Rissanen, M. Albrecht, *J. Am. Chem. Soc.* **2017**, 139, 16959–16966; b) M. A. Strauss, H. A. Wegner, *Angew. Chem. Int. Ed.* **2019**, 58, 18552–18556; *Angew. Chem.* **2019**, 131, 18724–18729.  
 [34] K. Szalewicz, *WIREs Comput. Mol. Sci.* **2012**, 2, 254–272.

- [35] a) J. M. Turney, A. C. Simmonett, R. M. Parrish, E. G. Hohenstein, F. A. Evangelista, J. T. Fermann, B. J. Mintz, L. A. Burns, J. J. Wilke, M. L. Abrams, N. J. Russ, M. L. Leininger, C. L. Janssen, E. T. Seidl, W. D. Allen, H. F. Schaefer, R. A. King, E. F. Valeev, C. D. Sherrill, T. D. Crawford, *WIREs Comput. Mol. Sci.* **2012**, *2*, 556–565; b) R. M. Parrish, L. A. Burns, D. G. A. Smith, A. C. Simmonett, A. E. DePrince, E. G. Hohenstein, U. Bozkaya, A. Y. Sokolov, R. Di Remigio, R. M. Richard, J. F. Gonthier, A. M. James, H. R. McAlexander, A. Kumar, M. Saitow, X. Wang, B. P. Pritchard, P. Verma, H. F. Schaefer, K. Patkowski, R. A. King, E. F. Valeev, F. A. Evangelista, J. M. Turney, T. D. Crawford, C. D. Sherrill, *J. Chem. Theory Comput.* **2017**, *13*, 3185–3197.
- [36] T. M. Parker, L. A. Burns, R. M. Parrish, A. G. Ryno, C. D. Sherrill, *J. Chem. Phys.* **2014**, *140*, 094106.
- [37] a) K. Carter-Fenk, J. M. Herbert, *Chem. Sci.* **2020**, *11*, 6758–6765; b) K. Carter-Fenk, J. M. Herbert, *Phys. Chem. Chem. Phys.* **2020**, *22*, 24870–24886.
- [38] a) W. B. Schneider, G. Bistoni, M. Sparta, M. Saitow, C. Riplinger, A. A. Auer, F. Neese, *J. Chem. Theory Comput.* **2016**, *12*, 4778–4792; b) A. Altun, M. Saitow, F. Neese, G. Bistoni, *J. Chem. Theory Comput.* **2019**, *15*, 1616–1632; c) A. Altun, F. Neese, G. Bistoni, *J. Chem. Theory Comput.* **2019**, *15*, 215–228.
- [39] F. Neese, *WIREs Comput. Mol. Sci.* **2018**, *8*, e1327.

Manuscript received: March 24, 2022

Accepted manuscript online: May 11, 2022

Version of record online: June 14, 2022